

Metric Tracking Services in the Era of Optical Communications

Gregory W. Heckler^{a*}, Anne Long^b, Luke B. Winternitz^c, Jennifer Donaldson^d, Guangning Yang^e

^a NASA Headquarters, 300 E Street SW in Washington D.C, 20546, 202.358.1626, gregory.w.heckler@nasa.gov

^b a.i. solutions, Inc., Lanham, MD 20706, 301.306.1756, anne.long@ai-solutions.com

^c NASA Goddard Space Flight Center, Greenbelt, MD 20771, 301.286.4831, luke.b.winternitz@nasa.gov

^d NASA Goddard Space Flight Center, Greenbelt, MD 20771, 301.614.7079, jennifer.e.donaldson@nasa.gov

^e NASA Goddard Space Flight Center, Greenbelt, MD 20771, 301.614.6806, guangning.yang-1@nasa.gov

* Corresponding Author

Abstract

The Space Communications and Navigation program, at the National Aeronautics and Space Administration, is developing free-space optical communications technology to facilitate the next generation of space missions in near-Earth, Lunar, and planetary space. A discussion of optometric observation performance and hardware-in-the-loop test results are presented. Simulation of orbit-determination for LEO and Lunar spacecraft relying on optometric tracking extends raw observation accuracy to realizable orbit-determination performance. Potential science and operational applications are reviewed, along with NASA's approach for developing optometric technology. Current investments in developing optometric hardware and plans for NASA's future optical communications network define the path for a future operational optometric capability in the 2020's and beyond.

Keywords: orbit determination, optical communications, metric tracking

Acronyms/Abbreviations

Consultative Committee on Space Data Standards (CCSDS)
Direct-to-Earth (DTE)
European Data Relay System (EDRS)
Geosynchronous Earth orbit (GEO)
Global Positioning System (GPS)
Global Navigation Satellite System (GNSS)
Goddard Space Flight Center (GSFC)
Goddard Enhanced Onboard Navigation System (GEONS)
Gravity Recovery and Climate Experiment Follow On (GRACE-FO)
Johnson Space Center (JSC)
Laser Communications Relay Demonstration (LCRD)
Laser Ranging Interferometer
Low Earth orbit (LEO)
Lunar Laser Communication Demonstration (LLCD)
National Aeronautics and Space Administration (NASA)
Near rectilinear halo orbit (NRHO)
Numerical controlled oscillator (NCO)
Orbit determination (OD)
Precise orbit determination (POD)
Radio frequency (RF)
Size weight and power (SWAP)
Small Business Innovation Research (SBIR)
Small Business Technology Transfer Program (STTR)
Space Communications and Navigation (SCaN)
Space Test Program Satellite-6 (STPSat-6)
Sun-synchronous orbit (SSO)

Tracking Data Relay Satellite (TDRS)

1. Introduction

The Space Communications and Navigation program, at the National Aeronautics and Space Administration, is developing free-space optical communications technology to facilitate the next generation of space missions in near-Earth, Lunar, and planetary space. Optical communication links can operate at data rates 10x – 100x higher than traditional microwave links, but with smaller terminal size, weight, and power requirements **Error! Reference source not found.** Currently NASA relies on microwave communication links to deliver radiometric tracking (range and range-rate/Doppler) observations for orbit determination of spacecraft and science applications. Optical communications technology offers an unheralded opportunity to generate metric tracking data accurate to 10s of nanometers, a 5 order of magnitude improvement over microwave based technologies [2].

Advances in signal processing techniques and space-rated hardware have made a transition from microwave to optical communication possible. Optical communication offers advantages which make its pursuit worthwhile, including:

1. Smaller user terminal size, weight, and power envelope
2. Low probability of intercept and probability of detection
3. Optical communications is currently unregulated, eliminating coordination through the FCC or NTIA (U.S. only)
4. 1550 nm optical communication hardware leverages commercial component supply chain
5. Access to multi-GHz of spectrum (~100s of GHz)

For those reasons listed, NASA sees a transition from the technology curve represented by traditional microwave communications to the technology curve optical communications. The technology space is rapidly maturing, with operational systems, such as the European Data Relay System [3], already in place and demonstrations of 200 gigabit-per-second (Gbps) direct-to-Earth (DTE) optical links from low-Earth-orbiting (LEO) spacecraft soon to be launched [4].

2. Attainable Optimetric Performance

The generation of navigation observables with optical communication systems is referred to as optimetrics. Two sources of navigation observation, the data clock and the optical carrier, are available on optical communication links. Observations of these two sources generate both range and range-rate tracking data. Orbit determination can be accomplished with range and/or range-rate observations, which are either one-way or two-way. Range measurements should be unambiguous or have an ambiguity interval large enough to be easily resolved.

Free-space optical communication requires closed loop pointing to microradian levels of accuracy. Fine pointing information is also a useful navigation observable but is not discussed in this paper.

At the physical layer the carrier frequency sets the highest fundamental frequency and bounds the precision of the observation. NASA’s current space communication services rely on microwave carriers in the S, X, or Ka bands, ranging from roughly 2 to 32 GHz. Dividing the speed of light, c , by the carrier frequency, f_c , generates the fundamental wavelength and provides an estimate for ranging performance:

Table 1: Ranging Performance Estimates

Fundamental Frequency (Hz)	1.023 MHz	2 GHz	26 GHz	193 THz
Fundamental Wavelength (m)	2.93E+02	1.50E-01	1.15E-02	1.55E-06
Ranging Precision	29.3 m	1.5 cm	1.15 mm	155 nm

Table 1 compares first order ranging performance estimates of communication systems with different fundamental frequencies. 1.023 MHz represents the chipping rate of the Global Positioning System’s Civilian Access code, which is transmitted on a 1.57542 GHz microwave carrier. It is conservative to assume a transceiver or transponder can measure to a precision of 10% of the fundamental wavelength. GPS receivers can apply carrier smoothing to the pseudorange observation but it requires successful carrier cycle ambiguity resolution. A receiver with carrier smoothing capability can deliver pseudorange precision relative to the 1.57542 GHz carrier instead of the 1.023 MHz CMDA code.

A space transponder able to receive a 2 GHz S-band carrier and resolve the carrier ambiguity is able to make range measurements with 1.5 cm of precision. NASA’s optical communication’s technology is based on commercial components that operate in the 1550 nm optical wavelength region. A 1550 nm wavelength corresponds to a fundamental frequency of 193 THz, and thus establishes 155 nm ranging precision as an achievable performance assumption.

Ranging performance is improved as a receiver can track and observe higher fundamental frequencies in the communications channel at the physical, link, and network levels. The optimetrics technique proposed in this paper relies on the medium, physical, and link layers of the optical communications stack to build a set of rulers, each with traceability to the previous ruler and with increasing precision.

3. Optimetric Techniques

Two techniques are proposed to generate range and range-rate observations. These techniques exploit information already in the communications channel without adding major requirements on the optical terminal. Note optical communications technology also offers an opportunity to exploit wavelength division multiplexing to dedicate optical spectrum to the generation of navigation observables. NASA sees this as unnecessary given the ability to generate range and range-rate observations with small changes to current implementation approaches.

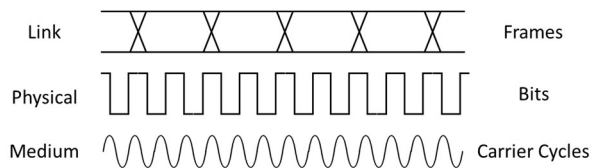


Figure 1. Generic Communication Stack

Figure 1 represents the three pertinent layers in the optical communications stack. Free space optical communication relies on modulation of the optical carrier. Modulation can be accomplished through various schemes, including on-off keying (OOK), pulse-position modulation (PPM), differential phase-shift keying (DSPK), or phase-shift keying (PSK) [5]. OOK, PPM, and DSPK modulations are non-coherent and do not require carrier phase detection and tracking by the receiving modem. PSK modulations require coherent detection and tracking of the incoming optical carrier phase.

The first technique is applicable to both non-coherent and coherent modulation schemes. This technique relies on demodulation of the bits and frame within the modem and is hence referred to as the “data clock” technique.

The primary optical terminal will modulate data bits onto the physical carrier. These bits are not arbitrary, they include repeating patterns with a known periodicity. Periodic frames can be forward error correction block codes or link layer data frames. As long as the frames are a fixed length and include an incrementing frame counter an unambiguous two-way range measurement can be generated.

The reference modem will have knowledge of the instantaneous frame count, bit count, and bit phase at the observation time. The secondary modem receives the incoming signal and coherently turns-around the received transmit data clock to the outgoing transmit data clock in both phase and frequency. The secondary modem must also transfer the state of the received frame count to the transmitted frame count. The reference modem can compare the entire state (both bits and frames) of the transmit clock to the receive clock. Differencing the transmit and received data clock states allows a range measurement to be generated. This process is illustrated in Figure 2:

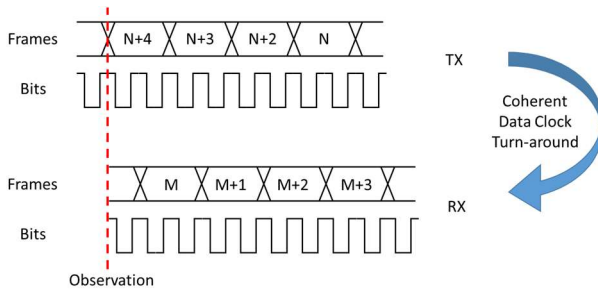


Figure 2. Data Clock Technique

The two way range observation is thus the difference of the received time, as computed from the received frame, bit, and partial bit count, with the transmit time, as computed from the transmitted frame, bit, and partial bit count.

$$\begin{aligned} \Delta_{frames} &= \text{full frame count difference} \\ \Delta_{bits} &= \text{full bit count difference} \\ \Delta_{bits} &= \text{single bit phase difference} \end{aligned}$$

$$r_{2way} = c * \left(\frac{\Delta_{frame}}{f_{frame}} + \frac{\Delta_{bits}}{f_{bits}} + \frac{\Delta_{bits}}{f_{bits}} \right) \quad (1)$$

As shown in Eq 1, the two way range is computed by scaling the sum of the difference in whole frames, whole bits, and partial bits appropriately to convert to meters. The ambiguity interval can be tuned by sizing the frame counter within the link layer frames appropriately.

One-way ranging can be accomplished by the insertion of time tags in the data stream by the reference modem. Ranging performance in this configuration will include additional errors from the reference and secondary modem’s knowledge of absolute time.

A two-way range-rate observation can be also computed by observation of received frames, bits, and partial bits, as in Eq 2.:

$$\begin{aligned} M_{frames} &= \text{instantaneous frame count} \\ K_{bits} &= \text{instantaneous bit count} \\ \phi_{bits} &= \text{instantaneous bit phase} \end{aligned}$$

$$\dot{r}_{2way} = \frac{c * \left(\frac{M_{frame}}{f_{frame}} + \frac{K_{bits}}{f_{bits}} + \frac{\phi_{clock}}{f_{bits}} \right)}{dt} \quad (2)$$

An integrated data clock count can be computed from the instantaneous frame, bit, and partial bit counters. This observation, when differenced, will correspond to the two-way range-rate between the reference and secondary modem.

To generate useable observations, the optical modems must fulfill the following requirements:

- 1) The modem’s TX and RX reference clocks must be coherent, i.e. derived from a common master oscillator
- 2) The reference modem must have knowledge of absolute time to time stamp the range and range-rate observation
- 3) The secondary modem must coherently track the received data clock and modulate the transmitted data with the recovered clock

The data clock technique’s accuracy is limited by the data rate on the optical link. Current optical data rates stretch from the 10’s of Mbps to 200 Gbps, translating to observation precision ranging from 3.0 m to 0.15 mm. This level of precision is comparable with RF methods that rely on observation of the microwave carrier.

Observation of the 1550 nm optical carrier will increase ranging precision into the nanometer regime. The challenge is to synchronize the optical carrier with the data clock, in the same way RF communication systems do today.

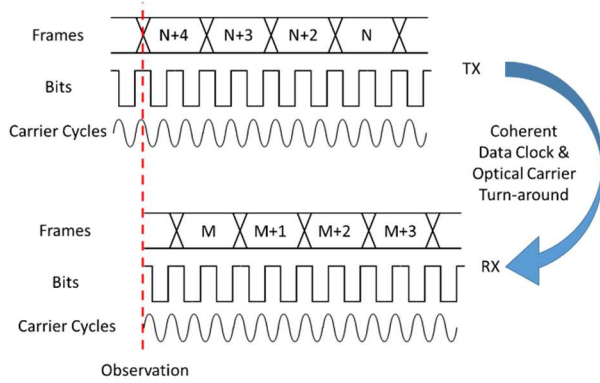


Figure 3. Optical Carrier Technique

If the modem is able to track and record observations of the carrier phase, along with the bit and frame counts, the two way range is calculated by the normalize sum of differences, as in Eq 3.:

$$\begin{aligned}
 \Delta_{frames} &= \text{full frame count difference} \\
 \Delta_{bits} &= \text{full bit count difference} \\
 \Delta_{cycles} &= \text{full carrier cycles} \\
 \Delta_{pha} &= \text{partial carrier cycle}
 \end{aligned}$$

$$r_{2way} = c * \left(\frac{\Delta_{frame}}{f_{frame}} + \frac{\Delta_{bits}}{f_{bits}} + \frac{\Delta_{cycles}}{f_{carrier}} + \frac{\Delta_{phase}}{f_{carrier}} \right) \quad (3)$$

Note an integrated carrier observation can be formed simply by maintaining an integration of the NCO used to maintain phase lock with the incoming optical carrier. The differential of this observation will generate an instantaneous two-way range-rate observation without requiring information from the frame or symbol synchronization processes.

Although simple in concept, synchronization of zero crossing of the optical carrier with the data clock requires additional hardware. Coherent generation of the bit and frame clocks from the optical carrier can be accomplished by an optical frequency comb. Optical combs generate very precisely spaced carriers centered about the main laser frequency. An optical comb passed into a photodiode will generate a microwave signal at the repetition frequency of the comb that is coherent to the original optical carrier. With proper design the resultant microwave signal can be generated with superior phase noise characterises over traditional microwave sources [6].

Optical modems often employ an intradyne receiver architecture, where the incoming optical signal is down converted by mixing with a reference laser [7]. The down converted signal is at a low enough center frequency to be processed by digital electronics clocked at MHz or GHz rates. Intradyne modems currently do not have a single coherent clock tree, the reference laser used to down convert the received signal is completely uncoupled from the clock which disciplines the digital signal processing circuitry.

An optical comb can be used to generate the digital signal reference clock directly from the reference laser. By doing so the electronics will be synchronized to the reference laser. Such a modem would allow for the observations necessary to fulfil Eq. 3.

4. Laboratory and Demonstration Performance

Experiments and demonstration of free-space optical communications in terrestrial and space applications are already underway. One such space mission was the Lunar Laser Communications Demonstration. In 2013 LLCD transmitted data at a rate of 622 Mbps from the Moon to the Earth. LLCD also demonstrated two-way ranging with a variation of the data clock technique. The LLCD ranging experiment resulted in two-way range measurements with residual noise of 0.94 cm (1-sigma) based on a 311 MHz system clock [8]. This measurement precision equates to <1% of the fundamental frequency and confirms the conservativeness of the 10% rule-of-thumb discussed in Section 2.

Lab experiments carried out at Goddard Space Flight Center after LLCD further explored both the data clock and optical carrier techniques. Measurement noise can be greatly reduced by adding an offset frequency to the data clock turned around by the secondary modem. An offset frequency allows the reference modem to more precisely measure the relative phase of the outgoing and incoming data clock. Guan et al. demonstrated 23.1 μm (1-sigma) ranging precision based on 622 Mbps system clock in a laboratory setting [9].

The same team implemented a demonstration of high precision ranging over a coherent optical communication link. By implementing the optical carrier optometric technique with a 10 Gbps PSK link, the team demonstrated ranging accuracy of 60 nm (1 sigma) for two-way range at a 1 second integration time. Ranging performance was insensitive to received E_b/N_0 , as long as the receiver maintained lock. The demonstration was carried out using commercially available fiber telecom components at 1550 nm.

5. Navigation Performance

Optical communications technology is expected to be adopted by NASA missions in the 2020's. Such users include Earth future observing missions and Lunar exploration missions such as the Lunar Gateway. With achievable optometric ranging performance clearly demonstrated in both flight and ground demonstrations, investigation of navigation performance using optometrics is the next step. Two types of users were simulated: a user in sun-synchronous orbit representing an Earth observing mission and a Lunar Gateway user in a near rectilinear halo orbit around the Moon. Both simulations assumed optical communications occurred regularly between the user and a constellation of optical relays in geosynchronous orbits. The simulation investigated on-board orbit determination performance using the GEONS extended Kalman filter [10].

Optometric 2-way range and Doppler measurement were simulated using the 2-way cross-link measurement models available in GEONS for three hypothetical optical relays with initial state at the current locations for TDRS-E, TDRS-W, and TDRS-Z. Near-continuous optometric tracking is available to the GEO optical relays except for exclusions when the vehicle is occulted by the Earth or Moon. The following tracking schedules were selected to provide schedules considered to be operationally realistic:

- For SSO: one 15-minute tracking contact per orbit
- For NRHO: three 15-minute tracking contacts per relay per day

The simulation compared standalone performance of optometric based orbit determination with standalone GPS performance and also a blended approach. Table 2 conveys the optometric observation performance assumed in the simulation, corresponding to a 10 Gbps data clock on the optical relay links:

Table 2: Optometric Observation Simulation Assumptions

	Value	Assumption
Baseline Range Noise (1-sigma)	0.030 m	rms random error <10% of a data clock cycle
Stretch Range Noise (1-sigma)	0.003 m	rms random error <1% of a data clock cycle
Range Bias	0.030 m	range measurement systematic residual error shall be less than 10% of a data clock cycle
Baseline Doppler Noise (1-sigma)	0.0255 Hertz	rms random error < 160 mrad/second
Stretch Doppler Noise (1-sigma)	0.0025 Hertz	rms random error < 16 mrad/second
Doppler Bias	0.0	
Relay State Errors	0.0	Relay orbit determination performed on the ground with high precision states provided to the user satellites.

GPS visibility is determined by a dynamic link budget with a 23 dB-Hz acquisition and tracking threshold for Lunar orbits and 35 dB-Hz for near Earth orbits. In the case of the SSO trajectory the GPS receiver model is based on the MMS-Navigator, but using an OCXO based on a Hi-Reliability Evacuated Miniature Crystal Oscillator (EMXO) OCXO [11]. In the case of the NRHO, the frequency reference was modeled using a model of a Spectratime Rubidium Atomic Frequency Standard (RAFS) [12]. Using the RAFS model, the time and frequency reference and distribution system maintains time to within 20 nanoseconds of a universal reference time scale (e.g. UTC or TAI); stability of $\leq 3e-13$ parts over time intervals of 10 seconds, $\leq 3.5e-14$ parts over time intervals of 1000 seconds, $\leq 1e-14$ parts over time intervals of 100,000 seconds (Hadamard Deviation).

The clock simulation model uses a twice integrated white noise model implemented in GEONS/Datagen. This is the same model used for the GPS clocks in the GPS MCS as described in [13].

Table 3: Dynamic Models Used in SSO Simulation

	Truth Trajectory Simulation	GEONS Filter Propagation with Nominal Dynamic Errors
Point Mass Gravity	Sun, Earth	Sun, Earth
Earth Joint Gravity Model (EGM96)	100x100	60x60
Solar Radiation Pressure Coefficient	$C_R = 2.0$	$C_R = 2.0 + 0.1 (1\sigma)$
Atmospheric Drag Coefficient	$C_D = 2.0$	$C_D = 2.0 + 0.1 (1\sigma)$
Propagation Algorithm, Stepsize	4 th order Runge-Kutta, 10 s	4 th order Runge-Kutta, 10 s

Table 3 outlines the dynamic model parameters used in the SSO simulation. The GEONS filter was configured to estimate the spacecraft position, velocity, time bias and time bias rate. The GEONS filter was initialized using an unconverged diagonal covariance matrix:

- RIC Position Covariance: 100^2 m^2
- RIC Velocity Covariance: $0.1^2 \text{ m}^2/\text{s}^2$
- Time Bias Covariance: 100^2 m^2
- Time Bias Rate Covariance: $0.1^2 \text{ m}^2/\text{s}^2$

Initial errors were randomly selected based on this covariance. Eight cases were investigated with different measurement observation sets. The RMS statistics from 40 Monte Carlo cases of the RSS position and velocity errors at the end of the simulation timespan are summarized in Table 4. Note that differences on the order of 0.1 m and 0.1 mm/s are not significant.

Table 4: SSO Navigation Performance

Simulation	Error Model	Optimetric Error Model	Mean RSS Position Error Final Day (m)	Mean RSS Velocity Error Final Day (mm/s)
GPS	Meas Only	N/A	0.33	0.39
GPS	Nominal	N/A	0.44	0.43
Optimetric	Meas Only	Baseline	0.43	0.45
Optimetric	Meas Only	Stretch Noise	0.38	0.42
Optimetric	Meas Only	Stretch Noise + 0.1*Range Bias	0.06	0.06
Optimetric	Nominal	Baseline	0.43	0.45
Optimetric + GPS	Meas Only	Baseline	0.11	0.13
Optimetric + GPS	Meas Only	Stretch Noise	0.12	0.11
Optimetric + GPS	Meas Only	Stretch Noise + 0.1*Range Bias	0.16	0.16
Optimetric + GPS	Nominal	Baseline	0.28	0.27

The SSO Monte Carlo simulations show that performing stand-alone OD using optimetrics is feasible, with the following observations:

- Steady-state accuracies at the submeter-level in position and tenth millimeter per second-level for velocity are achievable for a LEO satellite for all of the tracking configurations studied if high-fidelity dynamic models are implemented in the onboard orbit determination filter
- The addition of GPS measurements to optical tracking, significantly reduces the filter convergence time but provides a relatively small improvement in steady-state accuracy
- The reduction in the optical tracking random errors by a factor of 10 does not produce a significant improvement in steady-state accuracy because the

range bias, which remains at the baseline level, dominates the optical range measurement errors.

- Standalone optimetric navigation performance is at the same level as GPS only performance

The SSO OD performance was limited by dynamic modelling errors and the systemic residual error (bias) assumed in the ranging measurement. Further work with optical terminal engineers will be carried out to understand how to and to what accuracy end-to-end terminal delays can be calibrated. Dynamical modelling in the simulation also limited performance. Significant effort is expended by POD missions to model perturbation forces. Further simulation could investigate continuous optimetric tracking to determine if the dynamic modelling errors could be overcome by continuous observations.

Table 5: Dynamic Models Used in NRHO Simulation

	Truth Trajectory Simulation	GEONS Filter Propagation
Planetary Ephemeris	JPL DE 421	JPL DE 421
Point Mass Gravity	Sun, Earth, Venus, Mars, Jupiter, Saturn	Sun, Earth, Venus, Mars, Jupiter, Saturn
Lunar Gravity Model	30x30 LP150Q	30x30 LP100K
Solar Radiation Pressure	Spherical 24000 kg, 80 m ² , C _R = 1.0	Spherical 24000 kg, 80 m ² , C _R = 1.0 + 0.1 (1σ)

The nominal NRHO truth trajectory was simulated based on a JSC-provided ephemeris and used to compute 2-way optometric range and Doppler and GPS pseudorange measurements. This propagation was performed using operational software tools (AGI's STK/Astrogator) which are used by GSFC to support operational lunar, cis-lunar, and three-body dynamics missions. The same environmental models were used as used for the JSC ephemeris. Table 5 lists the modeling

for both the truth trajectory and the onboard navigation system (GEONS) used to simulate nominal dynamic errors. Differences include the lunar gravity model and solar radiation pressure to represent reality. In cases where nominal dynamic errors were not included, the same dynamic models were used to simulate the truth trajectory and in the GEONS filter.

The GEONS filter was configured to estimate the spacecraft position, velocity, time bias, time bias rate, and time bias acceleration. The GEONS filter was initialized using an unconverged diagonal covariance matrix:

- RIC Position Covariance: 100² m²
- RIC Velocity Covariance: 0.1² m²/s²
- Time Bias Covariance: 100² m²
- Time Bias Rate Covariance: 0.1² m²/s²
- Time Bias Acceleration Covariance: (3.6e-7)² m²/s⁴

The initial errors were randomly selected based on this covariance. For the NRHO analysis, eight cases were investigated with different measurement observation sets and dynamic error models. Table 6 summarizes the steady-state RMS statistics from 20 Monte Carlo samples. Note that for 20 samples, the full 90% confident limits are approximately 60% of the values shown.

Table 6: NRHO Navigation Performance

Measurement Set	Error Model	Optometric Errors	RSS Position Error Last Perilune (m)	RSS Velocity Error Last Perilune (mm/s)	RSS Position Error Last Apolune (m)	RSS Velocity Error Last Apolune (mm/s)
GPS	Meas. Only	N/A	4.81	1.30	2.02	0.1000
GPS	Nominal	N/A	18.77	5.20	13.79	0.2000
Optimetric	Meas. Only	Baseline	0.76	0.20	0.24	0.0020
Optimetric	Meas. Only	Stretch Noise	0.71	0.20	0.25	0.0020
Optimetric	Meas. Only	Stretch Noise +0.1*Range Biases	0.16	0.04	0.05	0.0010
Optimetric	Nominal	Baseline	33.57	9.30	13.10	0.0900
Optimetric + GPS	Meas. Only	Baseline	0.47	0.10	0.18	0.0020
Optimetric + GPS	Meas. Only	Stretch Noise	0.47	0.10	0.20	0.0020
Optimetric + GPS	Meas. Only	Stretch Noise +0.1*Range Biases	0.16	0.04	0.04	0.0010
Optimetric + GPS	Nominal	Baseline	9.03	2.50	5.00	0.1000

The simulation demonstrated that optometric navigation in an NRHO orbit is feasible, with the following observations:

- Solutions converge to steady-state performance after about 1 orbit. (6.5 days)
- Using 3-15 min contacts per day per relay with no dynamic errors and baseline optical relay measurement model, the steady-state RSS errors

remain below 2 m in position and 0.5 mm/s in velocity

- Dynamic modeling errors are the dominant error source. The peak errors, which are in the lateral direction, occur when the spacecraft is closest to the Moon. The magnitude of the peak errors is sensitive to the tracking schedule.

- Using 3-15 min contacts per day per relay with baseline dynamic errors and baseline optical relay measurement model, the steady-state RSS errors remain below 101 m in position and 19 mm/s in velocity
- Accuracies at the submeter-level in position and tenth millimeter per second-level for velocity are achievable for the NRHO at both apolune and perilune using two-way relay optometric measurements if there are no dynamic modeling errors. In this case, the addition of GPS measurements, decreases convergence time and provides a relatively small improvement in accuracy
- The GPS-only case takes at least 2 orbits to reach steady-state performance due to the time required to resolve the high correlation of the range position and time bias errors

Overall optometrics presents a feasible standalone OD solution for a spacecraft in NRHO orbit. Unlike the SSO simulation results, the blend of optometric and GPS tracking complemented each other and generated superior performance to the stand alone simulations. Optometric tracking performance was superior at apolune where dynamic disturbances are lower.

6. Development Plan

As NASA continues to develop optical communications technology it will formally incorporate optometrics as part of that capability. In 2020 NASA will start work within CCSDS to develop optical communication based ranging, Doppler, and time transfer standards. The initial standard will focus on the two techniques described in this paper but others may be proposed and incorporated as part of the standards process.

NASA has delivered and will operate the Laser Communications Relay Demonstration payload on the U.S. Air Force's Space Test Program Satellite-6. LCRD will demonstrate optical communication from geosynchronous orbit to two optical ground stations in California and Hawaii. The payload supports two different modulation schemes, DPSK at 1.244 Gbps and PPM at 311 Mbps. LCRD's first two years of flight will be dedicated to an experiment program. NASA has funded and is planning for an optometrics experiment to implement the data clock technique discussed in this paper. The experiment will not only investigate observation performance, but compare resulting orbit determination performance with STPSat-6's operational OD products.

NASA is also delivering an LCRD compatible user terminal, ILLUMA-T, to the International Space Station. This terminal will be capable of the data clock

turn around required to implement optometrics. It is expected that after the optometric experiment with LCRD and the two LCRD ground stations, an optometric experiment with LCRD and the ILLUMA-T terminal will provide the first space-to-space optometric test resulting in orbit determination for an optical comm space-relay user.

Further modem development is already underway to improve upon the technology flown on LCRD. GSFC is investigating optical modems that employ coherent PSK modulation to deliver 100 Gbps space-to-ground links and 10 Gbps space-to-space links. Lab testing with TRL5/6 modems that implement the data clock technique at these higher rates will be carried out in 2020. The optometric performance requirements identified in this paper were negotiated and vetted by the team focusing on the modem development.

The GSFC optical modem team is also leaning into the optical carrier technique. They are exploring laser components, including optical frequency combs and stabilized narrow-linewidth lasers, necessary to bridge the microwave the optical domains and create traceability between the optical carrier, data bits, and frames.

The data clock technique is already of high maturity and is on the path to operational infusion. Optometric requirements will be levied against future operational optical communication systems developed by NASA, likely in the early 2020s. The coherent optical technique is reliant on components that require further investment to reduce SWAP and to qualify them for space. NASA expects these capabilities to be available in the 2nd generation of operational optical communication service after 2025.

7. Applications

Optometrics provides an orbit determination capability not reliant on GPS. The use of GPS and GNSS by near-Earth spacecraft is rapidly becoming standard practice within the industry. Optometric tracking can provide either a stand-alone or backup capability to GPS based orbit determination to increase overall mission robustness and reliability. NASA is currently drafting policy stating that missions must have backup OD methods outside of GPS; optometrics will be a source of independent tracking data in the era of optical communications.

Precision orbit determination and time transfer are two obvious optometric applications. Although the performance investigated in this paper did not meet current POD capabilities or ~1 cm definitive orbit determination, the potential is still there. The navigation performance was affected by the ranging bias, which was assumed to be large relative the observation's precision. The ranging bias represents

uncalibrated delay within the reference and secondary modems. Further work with the modem experts will allow for reduction of this assumption through design and calibration. Improvement in the navigation simulation to more specifically simulate the OD process used for POD missions such as Jason-2 would also allow investigation of the benefit of optometric observations. Estimation of perturbation forces would of also improved performance.

For the coherent optical technique the ranging and Doppler performance identified in this paper is similar to the Laser Ranging Interferometer experiment flowing on the GRACE Follow On mission. GRACE-FO involves two spacecraft flying in formation using a microwave ranging system to detect changes in range and range-rate between the spacecraft. This information is used to sense the immediate gravity field. GRACE-FO included a new optical ranging demonstration. In this demonstration one spacecraft acts as the reference, sending out an optical carrier with stabilized frequency. The other spacecraft acts as a transponder and sends back an optical carrier that is coherent, but with a fixed 10 MHz offset, to the received optical signal. The requirement for the LRI ranging noise was set to $80 \text{ nm}/\sqrt{\text{Hz}}$ between 2 and 100 mHz. Early flight results show the LRI system exceeding the requirement [14]. If coherent optical ranging and Doppler observations become standard for all PSK optical links one could envision a “GRACE Everywhere” concept where observations from many spacecraft in orbit could improve the resolution and update rates of GRACE gravity maps. Such scientific results would be essentially “free” and a by-product of regular space operations.

A final application is envisioned where coherent optical communications technology is married to atomic optical clock technology. Optical clocks use many of the same laser components as coherent optical communication systems, including narrow linewidth lasers, cavity stabilized lasers, highly tunable lasers, and optical frequency combs to interrogate atomic species with transition lines in the optical domain. Optical atomic clocks offer unprecedented time and frequency stability characteristics over traditional microwave (Rb, Cs, H-maser) clocks [15]. Coherent optical links will allow time and frequency to be exchanged or disseminated from such clocks. NASA envisions using these technologies to allow small satellite missions to maintain coherency among the distributed apertures at both microwave and optical frequencies. Synthesizing such apertures from many small spacecraft will allow mission concepts and overall robustness not realizable by today’s large monolithic scientific spacecraft.

The long term performance advantages of optometrics is clear. The data clock technique provides

range and range-rate observables equal to or better than traditional microwave based observations and provides an important alternative to GPS based navigation for near Earth spacecraft. The true benefit of coherent optical communications, optometrics, and optical clocks will be realizable in the later 2020’s as the underlying technology components are redesigned for smaller SWAP, increased robustness, and survival in the space environment.

8. Discussion and Conclusion

NASA and SCA_N continue to invest in optical communications due to its performance and SWAP benefits over traditional microwave communications. As NASA pushes to explore Mars in the 2030’s the high data rate capabilities of optical communications will be required to meet the needs of humans in deep space. Coherent optical communication relies on the ability to acquire and track an optical carrier, and therefore is able to make phase and frequency observations of that carrier. Optical carrier observations generate a 4-5 order of magnitude improvement over current microwave techniques.

There is a clear infusion path for optometrics in the early 2020s as NASA fields initial instances of operational optical communications. The initial work carried out in the early 2020’s will allow for coherent optometrics to become an operational capability in the later half of the decade. NASA will continue to fund component level technology through direct funding and also the Federal SBIR and STTR programs.

Immediate work is necessary to translate optometric observation performance into system level orbit determination and time and frequency transfer performance. Further characterization of errors sources internal and external to the optical terminal are key in allowing OD performance on the same order as the underlying observation precision. This work will be carried out in concert with both navigation and optical communications experts to generate optometric requirements for the first generation of operational optical communication systems.

Acknowledgements

The authors would like to acknowledge Don Cornwell and Munther Hassounh for their help in facilitating the generation of this paper.

References

- [1] E. A. Park, D. Cornwell, D. Israel, "NASA's Next Generation ≥ 100 Gbps Optical Communications Relay", IEEE Aerospace Conference; March 02, 2019 - March 09, 2019
- [2] G. Yang, J. Chen, K. Numata, M. Krainak, G. Heckler and C. Gramling, "Optical carriers phase based high-precision ranging and range rate measurements in coherent optical communication," 2018 IEEE Aerospace Conference, Big Sky, MT, 2018, pp. 1-10
- [3] F. Heine, G. Mühlwinkel, H. Zech, S. Philipp-May and R. Meyer, "The European Data Relay System, High Speed Laser Based Data Links", 2014 7th Advanced Satellite Multimedia Systems Conference and the 13th Signal Processing for Space Communications Workshop (ASMS/SPSC), Livorno, 2014, pp. 284-286.
- [4] B. S. Robinson; D. M. Boroson; C. M. Schieler; F. I. Khatri; O. Guldner; S. Constantine; T. Shih; J. W. Burnside; B. C. Bilyeu; F. Hakimi; A. Garg; G. Allen; E. Clements; D. M. Cornwell, "TeraByte InfraRed Delivery (TBIRD): A Demonstration of Large-Volume Direct-to-Earth Data Transfer from low-Earth Orbit", Proc. SPIE 10524, Free-Space Laser Communication and Atmospheric Propagation XXX, 105240V (15 February 2018)
- [5] B. L. Edwards et al., "An update on the CCSDS optical communications working group," 2017 IEEE International Conference on Space Optical Systems and Applications (ICSOS), Naha, 2017, pp. 1-9.
- [6] S. A. Diddams et al., "Low jitter optical and microwave synthesis with frequency combs," 2010 IEEE International Topical Meeting on Microwave Photonics, Montreal, QC, 2010, pp. 409-411.
- [7] F. Derr, "Coherent optical QPSK intradyne system: concept and digital receiver realization," in Journal of Lightwave Technology, vol. 10, no. 9, pp. 1290-1296, Sept. 1992.[]
- [8] M. L. Stevens, R. R. Parenti, M. M. Willis, J. A. Greco, F. I. Khatri, B. S. Robinson, D. M. Boroson, "The lunar laser communication demonstration time-of-flight measurement system: overview, on-orbit performance, and ranging analysis," Proc. SPIE 9739, Free-Space Laser Communication and Atmospheric Propagation XXVIII, 973908 (15 March 2016)
- [9] G. Yang, W. Lu, M. Krainak and X. Sun, "High-precision ranging and range-rate measurements over free-space-laser communication link," 2016 IEEE Aerospace Conference, Big Sky, MT, 2016, pp. 1-13
- [10] NASA, Global Positioning System (GPS) Enhanced Onboard Navigation System (GEONS), <https://software.nasa.gov/software/GSC-14687-1/>, (accessed 07.10.2019)
- [11] Vectron, Hi-Reliability Evacuated Miniature Crystal Oscillator, 6/07/2019, <https://www.vectron.com/products/military/ocxo/EX-219.pdf>, (accessed 07.10.2019)
- [12] Spectratime, Rubidium Atomic Frequency Standard (RAFS), November 2016, https://www.spectratime.com/uploads/documents/ispace/iSpace_RAFS_Spec.pdf, (accessed 07.10.2019)
- [13] S. T. Hutsell, W. G. Reid, Lt J. D. Crum, Lt H. S. Mobbs, and J. A. Buisson. "Operational Use of the Hadamard Variance in GPS", In Proceedings of the 28th Annual Precise Time and Time Interval Systems and Applications Meeting/Proceedings of the Institute of Navigation GNSS+, pp 201–214, December 1996.
- [14] GRACE-FO, In-Orbit Performance of the GRACE Follow-on Laser Ranging Interferometer, Klaus Abich et al., Phys. Rev. Lett. 123, 031101 – Published 19 July 2019
- [15] N. Hinkley, J. A. Sherman, N. B. Phillips, M. Schioppo, N. D. Lemke, K. Beloy, M. Pizzocar, C. W. Oates, A. D. Ludlow, "An Atomic Clock with 10–18 Instability", Science, Sep 2013, pp 1215-1218